J Solid State Electrochem (2009) 13:921–926
DOI 10.1007/s10008-008-0629-9

ORIGINAL PAPER

Structural and electrochemical characterization of $LiFePO_4$/C prepared by a sol–gel route with long- and short-chain carbon sources

Xueliang Li · Weidong Wang · Chengwu Shi · Hua Wang · Yan Xing

Received: 9 June 2008 / Revised: 8 July 2008 / Accepted: 11 July 2008 / Published online: 1 August 2008

Abstract A fast and convenient sol–gel route was developed to synthesize $LiFePO_4$/C composite cathode material, and the sol–gel process can be finished in less than an hour. Polyethyleneglycol (PEG), D-fructose, 1-hexadecanol, and cinnamic acid were firstly introduced to non-aqueous sol–gel system as structure modifiers and carbon sources. The samples were characterized by X-ray powder diffraction, field emission scanning electron microscopy, and elemental analysis measurements. Electrochemical performances of $LiFePO_4$/C composite cathode materials were characterized by galvanostatic charge/discharge and AC impedance measurements. The material obtained using compound additives of PEG and D-fructose presented good electrochemical performance with a specific capacity of 157.7 mAh g^{-1} at discharge rate 0.2 C, and the discharge capacity remained about 153.6 mAh g^{-1} after 50 cycles. The results indicated that the improved electrochemical performance originated mainly from the microporous network structure, well crystalline particles, and the increased electronic conductivity by proper carbon coating (3.11%).

Keywords $LiFePO_4$/C · Sol–gel · Carbon sources · Characterization · Electrochemical performances

X. Li · W. Wang · C. Shi · H. Wang · Y. Xing
School of Chemical Engineering, Hefei University of Technology, Hefei, Anhui 230009, China

X. Li (✉) · W. Wang · C. Shi · H. Wang · Y. Xing
Anhui Key Laboratory of Controllable Chemical Reaction and Material Chemical Engineering, Hefei University of Technology, Hefei, Anhui 230009, China
e-mail: xueliangli2005@163.com

Introduction

Since Padhi et al. [1] proposed the electrochemical activity of $LiFePO_4$, olivine-type $LiFePO_4$ has been actively investigated as cathode material for Li ion secondary batteries [2–6]. $LiFePO_4$ has attracted great interest due to its low cost, environmental benignity, thermal stability, and high theoretical capacity.

In spite of these advantages, the olivine $LiFePO_4$ presents low conductivity (about 10^{-9} S cm^{-1}) [7, 8] and thereby its electrochemical performance is limited, resulting in poor rate capability. Improving and optimizing the electronic conductivity of $LiFePO_4$ becomes the key for application of this electrode material. Several groups dedicated their researches to resolving this problem [2, 9–14] via two main techniques. One is the reduction of the grain size of the sample and consequently the diminution of the diffusion length for both electrons and ions, and the other is the manufacture of $LiFePO_4$ coated with high conductivity carbon [4, 13–16].

Various approaches were studied to synthesize $LiFePO_4$/C, such as solid-state reaction [17], co-precipitation [5], hydrothermal synthesis [18], and sol–gel route [16]. Due to the advantage of forming uniform distribution and porous structure, sol–gel route attracted much attention. Meanwhile, sol–gel route can effectively inhibit the particle aggregation and facilely implement carbon coating of $LiFePO_4$ [3, 19, 20].

In fact, media can make crucial influences on gel time and the structure of xerogel (precursor) in sol–gel process. Though many great efforts have been made in the development of aqueous sol–gel route, it is difficult to conquer the drawback of its long time for gel and desiccation processes [21–23]. Therefore, it is necessary to develop new sol–gel systems. Non-aqueous solution may

play a key role on adjusting reaction time and improving xerogel structure. Therefore, an ethanol-based sol–gel route was developed to synthesize $LiFePO_4$/C composite cathode material in this paper. The whole sol–gel process needs only about 1 h, much less than conventional sol–gel time.

Many kinds of carbon sources have been reported for the $LiFePO_4$/C composite cathode material, e.g., sucrose [15], carbon black [24, 25], resorcinol-formaldehyde carbon aerogel [26], citric acid [27, 28], lauric acid [20], and polymeric additive [29–31]. However, to the best of our knowledge, there are still few reports on the synthesis of $LiFePO_4$/C composite cathode material with adding mixed carbon sources. In this paper, PEG (long chain), D-fructose, 1-hexadecanol, and cinnamic acid were firstly introduced to non-aqueous sol–gel system as the structure modifiers and mixed carbon sources. Structure and electrochemical performances of $LiFePO_4$/C were characterized by X-ray diffraction (XRD), field emission scanning electron microscopy (FE-SEM), AC impedance, and galvanostatic charge/discharge measurements.

Experimental

Sample synthesis

Metallic lithium was purchased from China Energy Lithium Co., Ltd and the other analytical chemicals were purchased from Shanghai Chemical Reagents Company and used without further purification and treatment.

The $LiFePO_4$/C composite cathode material was prepared by a fast and convenient sol–gel approach. As precursors, ferrous chloride tetrahydrate (0.1 mol) and lithium chloride monohydrate (0.1 mol) were dissolved separately in absolute ethanol to yield a 1 M solution and then mixed together. Phosphoric acid (0.1 mol) was added into the mixed solution slowly with moderate stirring, and following that, PEG (molecular weight of 1000) (4 g) and D-fructose (4 g) were dissolved in 50 ml absolute ethanol and added to the mixed solution. Then, this mixture was stirred slowly and heated slightly until the gel was formed. The resulting gel precursor was dried in an air oven at 60 °C, and after that, the precursor was decomposed at 350 °C for 4 h in flowing N_2 gas. Obtained powder was slightly ground and then sintered at 700 °C for 8 h in flowing N_2 gas.

For comparison, $LiFePO_4$/C with other mixed carbon sources (PEG and 1-hexadecanol, PEG and cinnamic acid) were also synthesized by the same sol–gel process. For convenient expression, we marked $LiFePO_4$/C with PEG and D-fructose as sample (A), $LiFePO_4$/C with PEG and 1-hexadecanol as sample (B), $LiFePO_4$/C with PEG and cinnamic acid as sample (C), and $LiFePO_4$ without any additive as sample (D), respectively.

Characterization

The residual carbon content of the powders was determined by means of an elemental analyzer (EA, Elementar Vario EL III). X-ray powder diffraction characterization was performed on a Japan Rigaku D/Max-rB diffractometer Cu-Ka radiation (λ=0.15406 nm) and graphite monochromator. FE-SEM characterizations of the samples were performed on an FEI (Sirion 200 and JSM-6700F) scanning electron microanalyzer. Electrochemical performances of the as-prepared materials were tested by assembling CR2032 coin cells. The positive electrodes were fabricated by pasting slurries of the as-prepared materials (85 wt.%), acetylene black (10 wt.%), and polyvinylidene fluoride (5 wt.%) dissolved in *N*-methyl-2-pyrrolidone on Al foil circular flakes. Then, the flakes were dried at 120 °C for 12 h in a vacuum drying oven. The value of loading density of positive electrode was 16–18 mg cm^{-2}. Metallic lithium was used as negative electrodes. The electrolyte was 1 M $LiPF_6$ in 1:1 ethylene carbonate and diethyl carbonate electrolyte, and the separator was Celgard 2400 micro-porous polypropylene membrane. The cells were assembled in a dry glove box filled with highly pure argon gas (O_2 and H_2O levels <1 ppm). Electrochemical impedance measurements were carried out by applying alternating voltage in the frequency range of 0.01 Hz to 100 kHz with amplitude of 5 mV on CHI-660B electrochemical workstation. The galvanostatic charge–discharge test was conducted by a BTS-55 Neware battery testing system at a current of 0.2–2 C with cutoff voltages of 2.5–4.2 V (vs. Li/Li^+) at room temperature.

Results and discussion

XRD analysis

X-ray diffraction patterns of $LiFePO_4$ are shown in Fig. 1. All diffraction peaks can be attributed to $LiFePO_4$ with an ordered olivine structure indexed by orthorhombic Pnma (JCPDS card No. 81-1173). The crystallite size D was calculated using the Scherrer's equation: $\beta\cos(\theta) = \kappa\lambda/D$, where β is the full-width at half-maximum length of the diffraction peak on a 2θ scale and κ is a constant (0.9). From the Scherrer's equation, D values for sample (A), (B), (C), and (D) were found to be 52, 67, 60, and 76 nm, respectively. As shown in Fig. 1, no evident impurities were detected in all samples. The amounts of residual carbon in sample (A), (B), (C), and (D) were 3.11%, 4.28%, 3.55%, and 0.37%, respectively. However, we cannot find any diffraction peak attributed to carbon, which is probably due to the amorphous or low crystalline of carbon in samples.

The lattice constants of all samples are shown in Table 1. There was no obvious change for lattice constants of

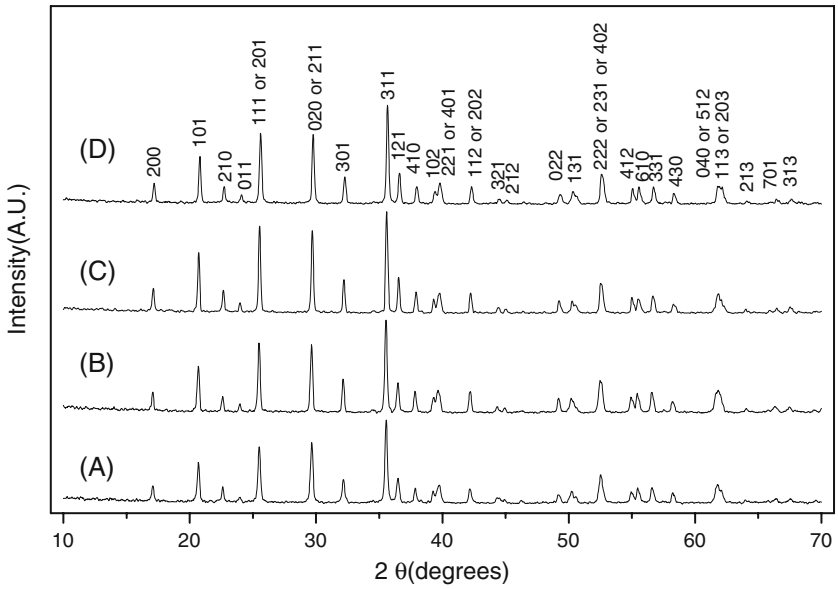

Fig. 1 XRD patterns of samples synthesized with PEG and D-fructose (**a**); with PEG and 1-hexadecanol (**b**); with PEG and cinnamic acid (**c**); without additive (**d**)

samples with different compound additives, and comparing with sample (D) without additive, the lattice constants and cell volumes of other samples were on slight downward trends.

Morphology

SEM images of samples are shown in Fig. 2. Sample (A) synthesized with PEG and D-fructose presented microporous network structure. This morphology may greatly improve the electrochemical performances for lithium ion battery, for the microporous network structure could enhance the electronic conductivity of the materials and increase contact surface area between particles and electrolyte. Sample (C) synthesized with PEG and cinnamic acid also exhibited regular morphology with approximately globular structure. The sizes of most particles estimated from Fig. 2c were in the range of 100–200 nm. The sample (B) synthesized with PEG and 1-hexadecanol consisted of globular and agglomerated particles. Meanwhile, the particles of both sample (B) and (C) formed loose connection, respectively. However, the particles of sample (D) congregated together and grew up to larger and non-uniform agglomerated particles. This irregular morphology of sample (D) was attributed to the lack of additive. The tapped densities of samples (A), (B), (C), and (D) were 1.47, 1.43, 1.35, and 1.56 g cm^{-3}, respectively.

SEM and XRD results indicated that the samples synthesized with compound additives facilely presented regular porous morphology and smaller particle size. In the sol–gel process, the carbon sources became to be part of precursor molecule. When heated, the organic part of the precursor would decompose to carbon with metal ions and phosphate radically distributed around it uniformly. The residual carbon would limit the growth of the particles and block the agglomeration of $LiFePO_4$ during the sintering process.

The compound additives consisted of long- and short-chain organic molecules in sample (A); the decomposition temperature of short-chain organic molecule is below that of long-chain organic molecule. D-Fructose decomposes at 105 °C, while PEG decomposes at above 300 °C under N_2 atmosphere. The compound additives decomposed step by step might play a key role on maintaining the particular structure of final products. As seen from Fig. 2b, c, with increasing of decomposition temperature, additives presented lower ability in forming network structure. 1-Hexadecanol and cinnamic acid, decomposing at 344 and 300 °C, respectively, did not result in the particular morphology as D-fructose did. The result indicated that the compound additives acted not only as carbon sources but also as structure modifiers in the synthesis.

Table 1 The lattice constants and cell volumes of sample (A), (B), (C), and (D)

Samples	Lattice constants (Å)			Cell volume(Å^3)
	a	*b*	*c*	
(A)	10.310	6.005	4.703	291.17
(B)	10.316	6.001	4.707	291.39
(C)	10.312	6.007	4.702	291.26
(D)	10.325	6.006	4.708	291.95

Electrochemical properties

Figure 3 shows the charge/discharge profiles of $LiFePO_4$ synthesized with and without additive, respectively. Typical

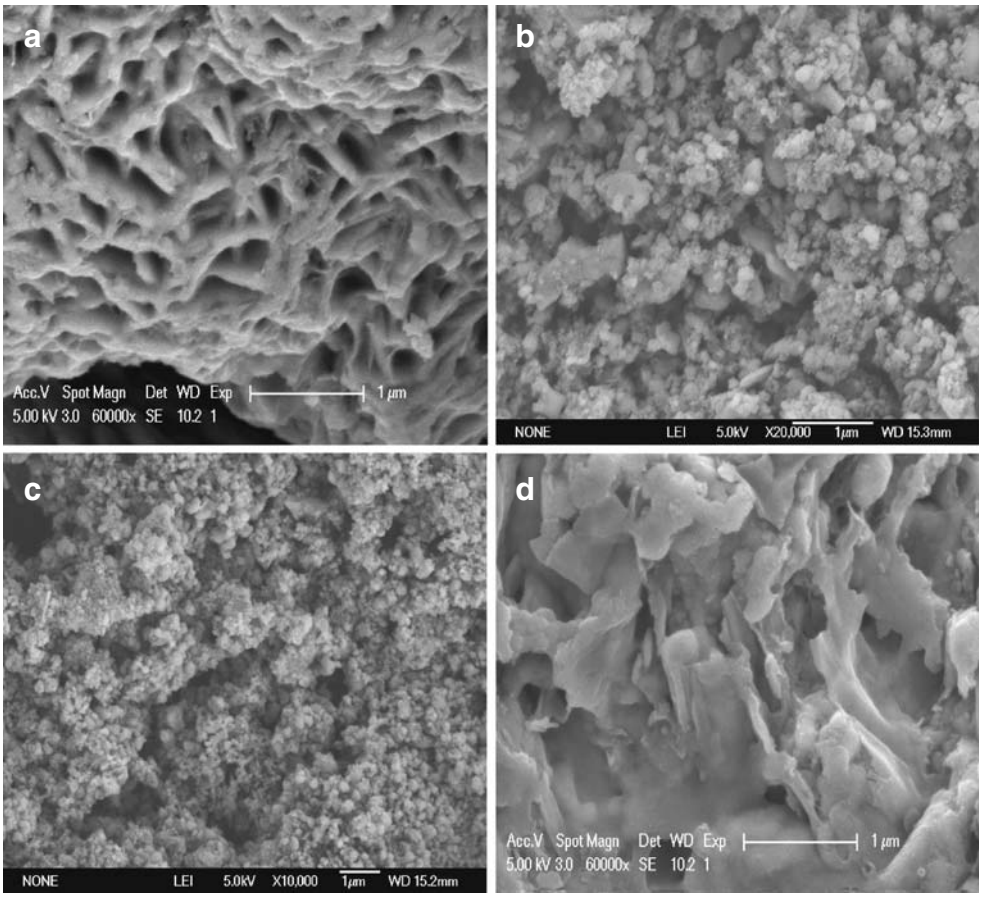

Fig. 2 SEM micrographs of samples synthesized with PEG and D-fructose (**a**); with PEG and 1-hexadecanol (**b**); with PEG and cinnamic acid (**c**); without additive (**d**)

flat plateaus around 3.4 V are observed during both charge and discharge in the curves of $LiFePO_4$/C synthesized with additives, which correspond to the reaction:

$$LiFePO_4 \Leftrightarrow (1-x)LiFePO_4 + xLi^+ + xFePO_4 + xe^-$$

As shown in Fig. 3, the sample (D) shows a specific capacity of 116.0 mAh g^{-1}, while samples (A), (B), and (C) deliver relatively high discharge specific capacity of more than 137.1 mAh g^{-1}. Obviously, the introduction of additives results in the increase of discharge specific capacity. Especially, $LiFePO_4$/C composite material prepared with PEG and D-fructose has the highest discharge-specific capacity of 157.7 mAh g^{-1} in all samples. In addition, the voltage separation during the charge/discharge process of the sample is much less than that of the sample synthesized without additive.

The results of charge/discharge test, SEM, and EA indicated that the improved electrochemical performance of $LiFePO_4$/C synthesized with additives resulted mainly from optimized amount of residual carbon in samples, uniform carbon coating, and appropriate porous network structure.

From Figs. 4 and 5, it can be seen clearly that the sample with additives exhibited higher discharge capacity and lower capacity loss ratio. Sample (A) presented good electrochemical performance with a reversible capacity of 130.9 and 157.7 mAh g^{-1} at discharge rates of 1 and 0.2 C, respectively, and the discharge capacity remained about 153.6 mAh g^{-1} after 50 cycles at 0.2 C. The capacity loss ratio of sample (A) was 0.05% per cycle; however, the

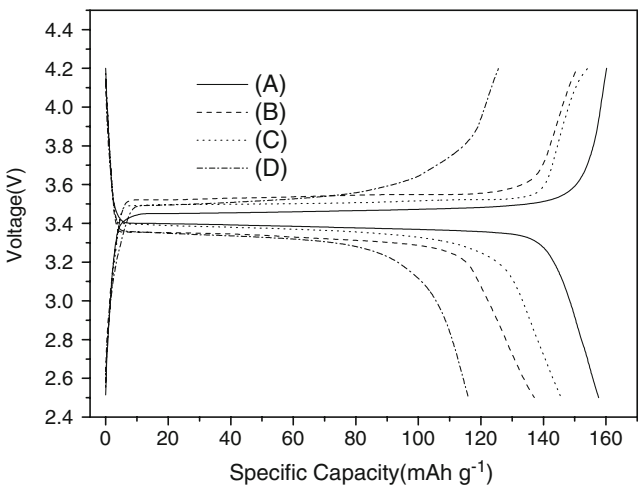

Fig. 3 The charge/discharge profiles at current density 34 mA g^{-1} (0.2 C) at room temperature for $LiFePO_4$ synthesized with PEG and D-fructose (**a**); with PEG and 1-hexadecanol (**b**); with PEG and cinnamic acid (**c**); without additive (**d**)

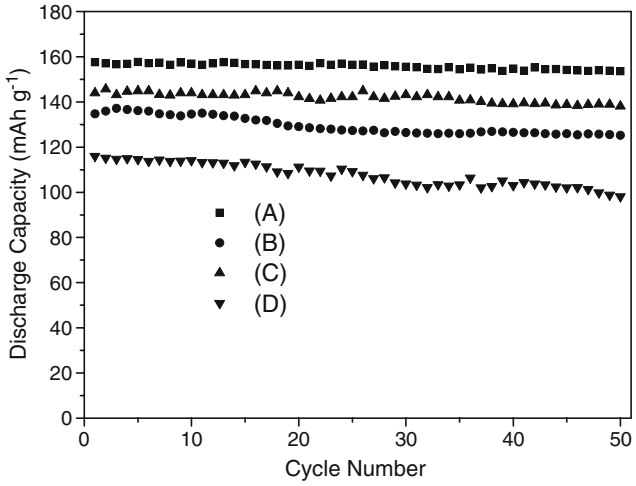

Fig. 4 Discharge capacity vs. cycle number at current density 34 mA g^{-1} (0.2 C) at room temperature of $LiFePO_4$ synthesized with PEG and D-fructose (**a**); with PEG and 1-hexadecanol (**b**); with PEG and cinnamic acid (**c**); without additive (**d**)

value of sample (D) rose to 0.3%, meaning that the existence of long- and short-chain carbon sources could improve reversible capacity and electrochemical stability.

Impedance analysis

The typical electrochemical impedance spectra of $LiFePO_4$ electrodes are presented in Fig. 6. The spectra showed an intercept at high frequency, followed by a semicircle in the high-middle frequency region, and a straight line in the low frequency region. The intercept impedance on the Z'-axis represented the solution resistance, which consisted of the resistance of the electrolyte and electrode. As shown in Fig. 6, the resistance of the combination of the electrolyte and electrode was similar for different $LiFePO_4$ electrodes. Possibly, this result was due to the additive of conductive carbon black.

The high frequency region of the semicircle represented the migration of the Li^+ ions at the electrode/electrolyte interface through the SEI layer, whereas the middle frequency range of the semicircle corresponded to the charge-transfer process. The low frequency region of the straight line was attributed to the diffusion of the lithium ions into the bulk of the electrode material or so-called Warburg diffusion.

From Fig. 6, it can be seen that the $LiFePO_4$/C composite materials synthesized with additives exhibited much lower charge-transfer resistance (81.31–190.9 Ω) than that (468.5 Ω) of the $LiFePO_4$ without additive. The decreases of charge-transfer resistance originated mainly from the increases of electronic conductivity and specific surface area, and mixed carbon sources play a key role in increasing electronic conductivity and specific surface area. Consequently, the long- and short-chain carbon sources can significantly increase the electrical conductivity and decrease charge-transfer resistance.

The particles of sample (A) were enwrapped by carbon network, leading to better utilization of the active materials and better capacity retention on cycling.

The performance including excellent cycling characteristics and low charge-transfer resistance confirmed the key role of structure and morphology, such as small particle size, porous network, and appropriate residual carbon. Meanwhile, the good rate capability was realized by improving electronic conductivity via effective carbon coating.

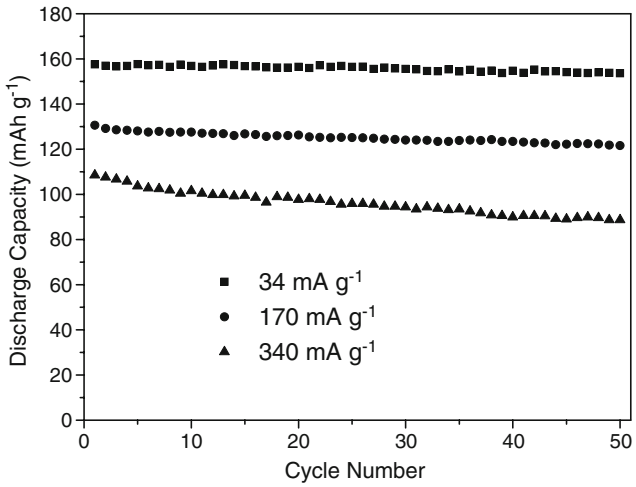

Fig. 5 Cycle life at different current densities from 34 mA g^{-1} (0.2 C) to 340 mA g^{-1} (2 C) at room temperature of the sample (A) synthesized with PEG and D-fructose

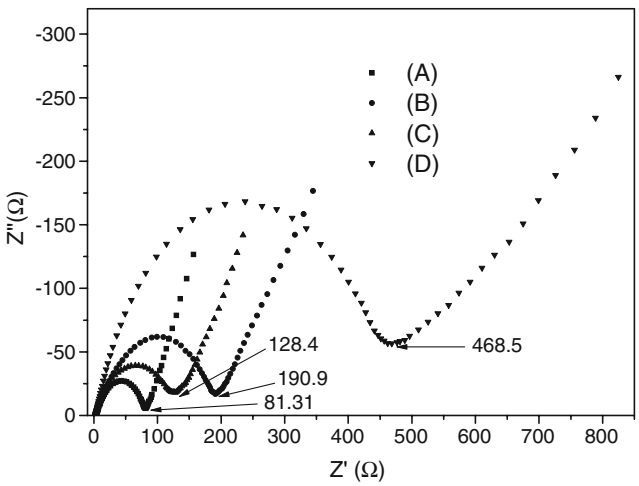

Fig. 6 Impedance spectra of the samples synthesized with PEG and D-fructose (**a**); with PEG and 1-hexadecanol (**b**); with PEG and cinnamic acid (**c**); without additive (**d**)

Conclusions

Uniform and fine particles of $LiFePO_4$/C were synthesized via a fast and convenient ethanol-based sol–gel route. Non-aqueous system provided a simple and fast approach to form and dry gel, and the sol–gel process can be finished in less than an hour. The $LiFePO_4$/C obtained using PEG and D-fructose exhibited best electrochemical performance in all samples with a specific capacity of 130.9 and 157.7 mAh g^{-1} at discharge rates of 1 and 0.2 C, respectively, and the discharge capacity remained about 153.6 mAh g^{-1} after 50 cycles at 0.2 C. The long- and short-chain carbon sources efficiently decreased particle size, formed homogeneous particular structure, and implemented uniform carbon coating. The additives played a key role on improving specific capability and its retention on cycling.

Acknowledgments This work was financially supported by the 2007 Annual Key Project of Anhui Province of China (No. 07020203003) and Major Scientific and Technological Issues of Anhui Province of China (No. 07010202032).

References

1. Padhi AK, Nanjundaswamy KS, Goodenough JB (1997) J Electrochem Soc 144:1188 10.1149/1.1837571
2. Herle PS, Ellis B, Coombs N, Nazar LF (2004) Nat Mater 3:147 10.1038/nmat1063
3. Dominko R, Bele M, Goupil JM, Gaberseek M, Hanzel D, Arcon L et al (2007) Chem Mater 19:2960 10.1021/cm062843g
4. Wilcox JD, Doeff MM, Marcinek M, Kostecki R (2007) J Electrochem Soc 154:A389 10.1149/1.2667591
5. Ong CW, Lin YK, Chen JS (2007) J Electrochem Soc 154:A527 10.1149/1.2720714
6. Gaberscek M, Kuzma M, Jamnik J (2007) Phys Chem Chem Phys 9:1815 10.1039/b618822b
7. Yamada A, Hosoya M, Chung SC, Kudo Y, Hinokuma K, Liu KY et al (2003) J Power Sources 119:232 10.1016/S0378-7753(03)00239-8
8. Chung SY, Bloking JT, Chiang YM (2002) Nat Mater 1:123 10.1038/nmat732
9. Fey George TK, Lu TL, Wu FY, Li WH (2008) J Solid State Electrochem 12:825 10.1007/s10008-008-0516-4
10. Thackeray M (2002) Nat Mater 1:81 10.1038/nmat736
11. Shi SQ, Liu LJ, Ouyang CY, Wang DS, Wang ZX, Chen LQ et al (2003) Phys Rev B 68:5
12. Gaberscek M, Dominko R, Bele M, Remskar M, Jamnik J (2006) Solid State Ionics 177:3015 10.1016/j.ssi.2006.07.060
13. Ellis B, Herle PS, Rho YH, Nazar LF, Dunlap R, Perry LK et al (2007) Faraday Discuss 134:119 10.1039/b602698b
14. Nakamura T, Miwa Y, Tabuchi M, Yamada Y (2006) J Electrochem Soc 153:A1108 10.1149/1.2192732
15. Bewlay SL, Konstantinov K, Wang GX, Dou SX, Liu HK (2004) Mater Lett 58:1788 10.1016/j.matlet.2003.11.008
16. Doeff MM, Hu YQ, McLarnon F, Kostecki R (2003) Electrochem Solid-State Lett 6:A207 10.1149/1.1601372
17. Kim DK, Park HM, Jung SJ, Jeong YU, Lee JH, Kim JJ (2006) J Power Sources 159:237 10.1016/j.jpowsour.2006.04.086
18. Dokko K, Koizumi S, Sharaishi K, Kanamura K (2007) J Power Sources 165:656 10.1016/j.jpowsour.2006.10.027
19. Xu ZH, Xu L, Lai QY, Ji XY (2007) Mater Res Bull 42:883 10.1016/j.materresbull.2006.08.018
20. Choi D, Kumta PN (2007) J Power Sources 163:1064 10.1016/j.jpowsour.2006.09.082
21. Piana M, Cushing BL, Goodenough JB, Penazzi N (2003) Ann Chim–Rome 93:985
22. Hsu KF, Tsay SY, Hwang BJ (2005) J Power Sources 146:529 10.1016/j.jpowsour.2005.03.094
23. Dominko R, Bele M, Gaberscek M, Remskar M, Hanzel D, Goupil JM et al (2006) J Power Sources 153:274 10.1016/j.jpowsour.2005.05.033
24. Dominko R, Gaberscek M, Drofenik J, Bele M, Pejovnik S, Jamnik J (2003) J Power Sources 119:770 10.1016/S0378-7753(03)00250-7
25. Zaghib K, Shim J, Guerfi A, Charest P, Striebel KA (2005) Electrochem Solid-State Lett 8:A207 10.1149/1.1865652
26. Wang GX, Yang L, Bewlay SL, Chen Y, Liu HK, Ahn JH (2005) J Power Sources 146:521 10.1016/j.jpowsour.2005.03.201
27. Gaberscek M, Dominko R, Bele M, Remskar M, Hanzel D, Jamnik J (2005) Solid State Ionics 176:1801 10.1016/j.ssi.2005.04.034
28. Hsu KF, Tsay SY, Hwang BJ (2004) J Mater Chem 14:2690 10.1039/b406774f
29. Mi CH, Cao GS, Zhao XB (2005) Mater Lett 59:127 10.1016/j.matlet.2004.07.051
30. Yun NJ, Ha HW, Jeong KH, Park HY, Kim K (2006) J Power Sources 160:1361 10.1016/j.jpowsour.2006.02.097
31. Tajimi S, Ikeda Y, Uematsu K, Toda K, Sato M (2004) Solid State Ionics 175:287 10.1016/j.ssi.2003.12.033